Spin Transition in [Fe(DPEA)(NCS)$_2$], a Compound with the New Tetradentate Ligand (2-Aminoethyl)bis(2-pyridylmethyl)amine (DPEA): Crystal Structure, Magnetic Properties, and Mössbauer Spectroscopy

Galina S. Matouzenko,*,† Azzedine Bousseksou,‡ Sylvain Lecocq,§ Petra J. van Koningsbruggen,|| Monique Perrin,§ Olivier Kahn,|| and André Collet*,†

Laboratoire de stéréochimie et interactions moléculaires, École normale supérieure de Lyon, 46, allée d'Italie, 69364 Lyon cedex 07, France, Laboratoire de chimie de coordination du CNRS, 205, route de Narbonne, 31077 Toulouse cedex, France, Laboratoire de reconnaissance et organisation moléculaire, Université Claude Bernard-Lyon 1, 69622 Villeurbanne cedex, France, and Laboratoire des sciences moléculaires, Institut de chimie de la matière condensée de Bordeaux, 33608 Pessac, France

Received December 20, 1996[⊗]

The new spin transition compound [Fe^{II}(DPEA)(NCS)$_2$], where DPEA [(2-aminoethyl)bis(2-pyridylmethyl)amine] is a new tetradentate ligand, has been synthesized, and its structure, magnetic properties, and Mössbauer spectra have been investigated. The crystal structure has been determined by X-ray diffraction at 298 K. The compound crystallizes in the monoclinic system, space group is $P2_1/c$, with $Z = 4$, $a = 9.358(1)$ Å, $b = 11.812(2)$ Å, $c = 17.135(2)$ Å, and $\beta = 94.5(4)°$. The distorted [FeN$_6$] octahedron is formed from four nitrogen atoms belonging to DPEA and two provided by the *cis* thiocyanate groups. The two pyridine rings of DPEA are in *mer* positions. Each molecule is linked to its neighbors by hydrogen-bonding interactions as well as by numerous van der Waals contacts supposed to be responsible for the cooperativity of the system. Variable-temperature magnetic susceptibility measurements (20−290 K) have evidenced a relatively abrupt $S = 2 \rightleftharpoons S = 0$ transition centered at $T_{1/2} = 138$ K. The thermal variation of the high spin state fraction observed by Mössbauer spectroscopy is in agreement with that obtained from magnetic susceptibility measurements. The fitting of Mössbauer and magnetic data with the Ising-like model allowed us to determine the energy gap between the high-spin and low-spin states ($\Delta_{eff} = 835$ K) and to estimate the variation of the thermodynamic parameters upon spin transition. The calculated variations of enthalpy ($\Delta H = 6.76$ kJ mol^{-1}) and entropy ($\Delta S = 49$ J mol^{-1} K^{-1}) associated with the spin transition are in agreement with those previously observed for iron(II) spin-crossover compounds. The spin conversion is found to be close to a first-order phenomenon.

Introduction

High-spin (HS, $^5T_2$) ⇌ low spin (LS, $^1A_1$) transitions in iron(II) compounds have been extensively studied during the last two decades. Spin transitions can be induced by physical perturbations, such as changes in temperature or pressure, and by light irradiation. These effects are well documented and have been summarized in several reviews.[1] The current interest in this phenomenon is due to its possible application to molecular electronics[2] and to its implication in certain biological processes.[3] Several theoretical models have been developed to relate the characteristics of the spin transition to the electronic and vibrational properties of the considered material and particularly to its molecular structure.[4] The sensitivity of the spin state to small perturbations suggests that new coordination complexes exhibiting spin transition phenomena could be designed through a fine tuning of the ligands surrounding the metal. According to Toftlund,[1d] one of the possible strategies for engineering such spin transition systems rests on the use of ligands containing both aliphatic and aromatic nitrogen donor atoms. The combination in the same ligand of nitrogen atoms of different nature is expected to generate an intermediate ligand field force which in turn can produce conditions favoring spin-state interconversion. Numerous complexes containing such a combination of ligands have been described.[1a,d,5] Recently, we have used this approach successfully in the case of a pseudo-

* To whom correspondence should be addressed.
† École normale supérieure de Lyon (UMR CNRS and ENS-Lyon No. 117; chaire de l'Institut universitaire de France).
‡ CNRS (UP CNRS 8241).
§ Université Claude Bernard-Lyon 1 (ESA Q5078).
|| Institut de chimie de la matière condensée de Bordeaux.
⊗ Abstract published in *Advance ACS Abstracts,* May 15, 1997.

(1) (a) Goodwin, H. A. *Coord. Chem. Rev.* **1976**, *18*, 293. (b) Gütlich, P. *Struct. Bonding* **1981**, *44*, 83. (c) König, E.; Ritter, G.; Kulshreshtha, S. K. *Chem. Rev.* **1985**, *85*, 219. (d) Toftlund, H. *Coord. Chem. Rev.* **1989**, *94*, 67. (e) Zarembowitch, J.; Kahn, O. *New J. Chem.* **1991**, *15*, 181. (f) König, E. *Struct. Bonding.* **1991**, *76*, 51. (g) Gütlich, P.; Hauser, A.; Spiering, H. *Angew. Chem., Int. Ed. Engl.* **1994**, *33*, 2024. (h) Kahn, O. *Molecular Magnetism*; VCH: New York, 1993.
(2) Kahn, O.; Codjovi, E. *Phil. Trans. R. Soc. Lond. A* **1996**, *354*, 359.
(3) (a) Tang, S. C; Koch, S.; Papaefthymiou, G. C., Foner, S.; Frankel, R. B.; Ibers, J. A.; Holm, R. H. *J. Am. Chem. Soc.* **1976**, *98*, 2412. (b) Morishima, I.; Iizuka, T. *J. Am. Chem. Soc.* **1974**, *96*, 5270. (c) Dose, E. V.; Tweedle, M. F.; Wilson, L. J.; Sutin, N. J. *J. Am. Chem. Soc.* **1977**, *99*, 3886. (d) Backes, W. L.; Sligar, S. G.; Schenkman, J. B. *Biochemistry* **1982**, *21*, 1324. (e) Ficher, M. T.; Sligar, S. G. *Biochemistry* **1987**, *26*, 4797.
(4) (a) Slichter, C. P.; Drickamer, H. G. *J. Chem. Phys.* **1972**, *56*, 2142. (b) Bari, R. A.; Sivardière, J. *Phys. Rev. B* **1972**, *5*, 4466. (c) Sasaki, N.; Kambara, T. *J. Phys. Soc. Jpn.* **1987**, *49*, 1806. (d) Sorai, M.; Seki, S. *J. Phys. Soc. Jpn.* **1972**, *33*, 575. (e) Bolvin, H.; Kahn, O. *Chem. Phys.* **1995**, *192*, 295. (f) Bousseksou, A.; Constant-Machado, H.; Varret, F. *J. Phys. 1 (Fr.)* **1995**, *5*, 747.
(5) (a) Toftlund, H.; Yde-Andersen, S. *Acta Chem. Scand. A* **1981**, *35*, 575. (b) Chang, H. R.; McCusker, J. K.; Toftlund, H.; Wilson, S. R.; Trautwein, A. X.; Winkler, H.; Hendrickson, D. N. *J. Am. Chem. Soc.* **1990**, *112*, 6814. (b) McCusker, J. K.; Toftlund, H.; Rheingold, A. L.; Hendrickson, D. N. *J. Am. Chem. Soc.* **1993**, *115*, 1797. (d) Al-Obaidi, A. H. R.; McGarvey, J. J.; Taylor, K. P.; Beel, S. E. J.; Jensen, K. B.; Toftlund, H. *J. Chem. Soc. Chem. Comm.* **1993**, 536. (e) McCusker, J. K.; Rheingold, A. L.; Hendrickson, D. N. *Inorg. Chem.* **1996**, *35*, 2100. (f) Al-Obaidi, A. H. R.; Jensen, K. B.; McGarvey, J. J.; Toftlund, H.; Jensen, B.; Beel, S. E. J., Carroll, J. G. *Inorg. Chem.* **1996**, *35*, 5055.

S0020-1669(96)01513-3 CCC: $14.00

Scheme 1[a]

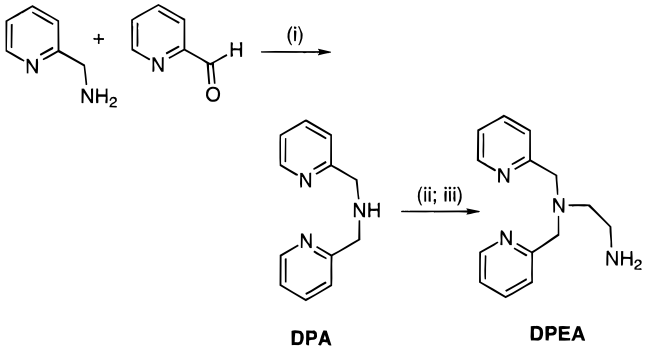

[a] Key: (i) Zn and AcOH in EtOH, 60−70 °C, 40%; (ii) *N*-(2-bromoethyl)phthalimide in toluene, 15 h reflux; (iii) hydrazine hydrate in EtOH, reflux, 41%.

Chart 1. Stereoisomers of $[Fe(DPEA)(NCS)_2]$[a]

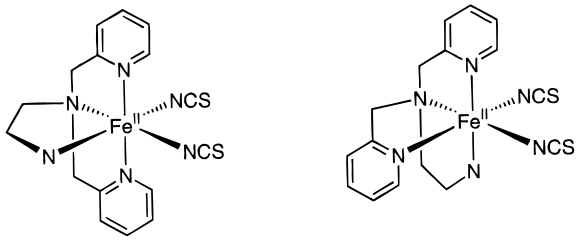

[a] Only **1**, where the pyridine ligands are meridionally arranged, was isolated in this work.

octahedral iron(II) complex of a C_3-cyclotriveratrylene ligand, for which different spin states have been found to coexist in the crystal lattice.[6]

In this paper we report the synthesis of (2-aminoethyl)bis-(2-pyridylmethyl)amine (DPEA), a new tetradentate ligand in which the conditions mentioned above are fulfilled (Scheme 1). This ligand was converted to the iron(II) complex $[Fe(DPEA)(NCS)_2]$ (**1**) (Chart 1), which showed a sharp spin transition centered at 138 K. The single-crystal X-ray structure, magnetic susceptibility, and Mössbauer spectroscopy of this complex were investigated, and the spin-state conversion was analyzed in the light of the Ising-like electron−vibrational model.[7] So far, cooperative spin transitions in *cis*-diisothiocyanatoiron(II) complexes have only been observed in $[FeL_2(NCS)_2]$, where L is a bidentate ligand (bipy, phen, etc.).[8] The $[FeL(NCS)_2]$ complexes of tetradentate ligands known before this work mainly give rise to spin equilibrium phenomena,[9] and none of these complexes have been characterized by X-ray crystallography.

Table 1. Crystallographic Data for $[Fe(DPEA)(NCS)_2]$

chem formula	$C_{16}H_{18}N_6S_2Fe$
a, Å	9.358(1)
b, Å	11.818(2)
c, Å	17.135(2)
α, deg	90.0(5)
β, deg	94.5(4)
γ, deg	90.0(5)
V, Å^3	1889(1)
Z	4
fw	414.33
space group	$P2_1/c$
temp, K	298
λ(Cu Kα), Å	1.540 56
ρ_{calc}, g·cm^{-3}	1.457
μ, cm^{-1}	85.63
R^a	0.066
$R_w{}^b$	0.073

[a] $R = \sum(|F_o| - |F_c|)/\sum|F_o|$. [b] $R_w = [\sum w(|F_o| - |F_c|)^2/\sum w|F_o|^2]^{1/2}$.

Experimental Section

Chemistry. All reagents and solvents used in this study are commercially available and were used without further purification. $[Fe(py)_4(NCS)_2]$ (py = pyridine) was prepared according to the described procedure.[10] All syntheses involving Fe(II) species were carried out in deoxygenated solvents under an inert atmosphere of N_2 using Schlenk type vessel or glovebox techniques. Elemental analyses (C, H, N, S, and Fe determinations) were performed at the Service Central de Microanalyse du CNRS in Vernaison, France. ^{1}H NMR spectra were recorded in $CDCl_3$ on a Bruker AC200 spectrometer operating at 200 MHz.

Ligand Synthesis. (a) Bis(2-pyridylmethyl)amine (DPA). A mixture of 2-(aminomethyl)pyridine (10.3 mL, 0.1 mol), zinc powder (20 g), and glacial acetic acid (20 mL) in 100 mL of 95% ethanol was vigorously stirred at 60−70 °C under argon. To this mixture, pyridine-2-carboxaldehyde (9.5 mL, 0.1 mol) was gradually added over a period of 2 h. Then further amounts of zinc powder (40 g) and glacial acetic acid (40 mL) were added over a period of 2 h, and stirring at 60−70 °C was continued for 5 h. The resulting mixture was allowed to stand at room temperature overnight, and the precipitate was filtered off. The filtrate was evaporated under reduced pressure to a syrup which was made alkaline with an excess of aqueous NaOH. The organic layer was extracted with ether, dried over $MgSO_4$, and evaporated to give a light brown oil which was distilled to give 8 g (40%) of a pale yellow syrup of DPA, bp 139−141 °C (1 Torr). ^{1}H NMR ($CDCl_3$): δ 8.52−7.04 (m, 8H, aromatic H's), 3.93 (s, 4H, CH_2), 2.55 (s, 1H, NH).

(b) (2-Aminoethyl)bis(2-pyridylmethyl)amine (DPEA). To a solution of the above DPA (8 g, 0.04 mol) in toluene (50 mL) were added 5.6 mL (0.04 mol) of triethylamine and 10.2 g (0.04 mol) of *N*-(2-bromoethyl)phthalimide. The mixture was refluxed under argon overnight and was then concentrated under reduced pressure. The solid residue was washed with 50 mL of cold water and then 50 mL of ether, to give 7.5 g (50%) of *N*-(2-(bis(2-pyridylmethyl)amino)ethyl)-phthalimide as a beige solid. ^{1}H NMR ($CDCl_3$): δ 8.43−7.00 (m, 8H, aromatic H's), 7.83−7.69 (m, 4H, aromatic H's), 3.84 (s, 4H, CH_2), 3.84−3.79 (t, 2H, CH_2), 2.89−2.81 (t, 2H, CH_2). To this product dissolved in 50 mL of absolute ethanol was added 0.98 mL (0.02 mol) of hydrazine monohydrate. The mixture was refluxed under argon until formation of a white gelatinous precipitate. When the formation of the latter appeared complete, it was decomposed by heating with 12 M HCl (8 mL). The precipitate (phthalyl hydrazide hydrochloride) was filtered off, and the solution was concentrated under vacuum. The residue was made basic with aqueous NaOH, and the organic material was extracted with ether. The ethereal solution was dried over KOH pellets and evaporated under vacuum, to give 4.1 g (41%) of practically pure DPEA (yellow oil). ^{1}H NMR ($CDCl_3$): δ 8.49−7.04 (m, 8H, aromatic H's), 3.76 (s, 4H, CH_2), 2.75−2.55 (m, 4H, CH_2), 1.45 (s, 2H, NH_2).

(6) Matouzenko, G.; Vériot, G.; Dutasta, J. P.; Collet, A.; Jordanov, J.; Varret, F., Perrin, M., Lecocq, S. *New J. Chem.* **1995**, *19*, 881.
(7) Bousseksou, A.; Nasser, J.; Linares, J.; Boukheddaden, K.; Varret, F. *J. Phys. 1 (Paris)* **1992**, *2*, 1381.
(8) (a) König, E.; Madeja, K.; Watson, K. J. *J. Am. Chem. Soc.* **1968**, *90*, 1146. (b) König, E.; Madeja, K. *Inorg. Chem.* **1967**, *6*, 48. (c) König, E.; Watson, K. J. *Chem. Phys. Lett.* **1970**, *6*, 457. (d) Sorai, M.; Seki, S. *J. Phys. Chem. Solids* **1974**, *35*, 555. (e) König, E.; Ritter, G.; Irler, W. *Chem. Phys. Lett.* **1979**, *66*, 336. (f) Ganguli, P.; Gütlich, P.; Müller, E. W. *J. Chem. Soc., Dalton Trans.* **1981**, 441. (g) Gallois, B.; Real, J. A. Hauw, C.; Zarembowitch, J. *Inorg. Chem.* **1990**, *29*, 1152. (h) Claude, R.; Real, J. A., Zarembowitch, J.; Kahn, O.; Ouahab, L.; Grandjean, D.; Boukheddaden, K.; Varret, F.; Dworkin, A. *Inorg. Chem.* **1990**, *29*, 4442. (i) Granier, T.; Gallois, B.; Gaultier, J.; Real, J. A.; Zarembowitch, J. *Inorg Chem.* **1993**, *32*, 5305. (j) Real, J. A.; Muñoz, M. K.; Andrés, E.; Granier, T.; Gallois, B. *Inorg. Chem.* **1994**, *33*, 3587.
(9) (a) Højland, F.; Toftlund, H.; Yde-Andersen, S. *Acta Chem. Scand. A* **1983**, *37*, 251. (b) Toftlund, H.; Pedersen, E.; Yde-Andersen, S. *Acta Chem. Scand. A* **1984**, *38*, 693. (c) Yu, Z.; Schmitt, G.; Böres, N.; Gütlich, P. *J. Phys.: Condens. Matter.* **1995**, *7*, 777. (d) Buchen, T.; Toftlund, H.; Gütlich, P. *Chem. Eur. J.* **1996**, *2*, 1129.
(10) Erickson, N. E.; Sutin, N. *Inorg. Chem.* **1966**, *5*, 1834.

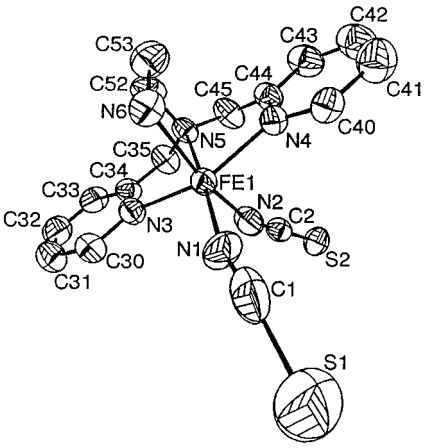

Figure 1. Perspective view of the [Fe(DPEA)(NCS)$_2$] molecule, showing the atom-numbering scheme. The ellipsoids enclose 50% probability.

Table 2. Fractional Atomic Coordinates and Isotropic Equivalent Displacement Parameters[a,b] for Non-Hydrogen Atoms of [Fe(DPEA)(NCS)$_2$]

atoms	*x*/*a*	*y*/*b*	*z*/*c*	B_{eq}
Fe1	0.05443(7)	0.17248(6)	0.36660(4)	3.39(1)
S1	0.3293(2)	−0.1638(2)	0.4284(1)	7.31(5)
N1	0.1546(4)	0.0179(3)	0.4008(3)	4.5(1)
C1	0.2242(6)	−0.0486(6)	0.4119(3)	5.3(1)
S2	0.2782(2)	0.1934(1)	0.12195(8)	5.44(3)
N2	0.1119(5)	0.1668(4)	0.2473(3)	5.6(1)
C2	0.1812(5)	0.1786(4)	0.1953(3)	4.1(1)
N6	−0.0003(6)	0.2190(4)	0.4859(3)	4.4(1)
C53	−0.0362(7)	0.3433(6)	0.4864(4)	5.8(2)
C52	−0.1233(7)	0.3717(5)	0.4152(4)	5.7(1)
N5	−0.0606(4)	0.3356(3)	0.3425(2)	4.09(9)
N3	−0.1681(4)	0.1239(3)	0.3355(2)	3.92(9)
C30	−0.2321(6)	0.0255(5)	0.3531(3)	4.7(1)
C31	−0.3747(7)	0.0061(6)	0.3375(4)	5.6(1)
C32	−0.4595(7)	0.0860(6)	0.3017(4)	6.0(2)
C33	−0.3975(5)	0.1882(6)	0.2823(3)	5.2(1)
C34	−0.2527(5)	0.2036(4)	0.3000(3)	4.1(1)
C35	−0.1753(7)	0.3124(5)	0.2809(4)	5.3(1)
N4	0.2242(4)	0.2979(3)	0.3848(2)	3.88(9)
C40	0.3544(5)	0.2805(6)	0.4213(3)	4.8(1)
C41	0.4563(7)	0.3631(7)	0.4307(4)	6.4(2)
C42	0.4212(8)	0.4694(8)	0.4014(4)	7.1(2)
C43	0.2891(8)	0.4899(6)	0.3669(4)	5.9(2)
C44	0.1898(6)	0.4021(5)	0.3580(3)	4.5(1)
C45	0.0461(7)	0.4163(5)	0.3145(4)	5.8(2)

[a] Estimated standard deviations in the least significant digits are given in parentheses. [b] $B_{eq} = {}^4/_3\sum_i\sum_j\beta_{ij}a_ia_j$.

Complex Synthesis. To 10 mL of a solution of [Fe(py)$_4$(NCS)$_2$] (48.8 mg, 0.1 mmol) in methanol was added 5 mL of an ethanol solution containing 24.2 mg (0.1 mmol) of DPEA. The resulting green brown solution was allowed to stand overnight at room temperature, to give yellow brown prismatic crystals of **1** which were collected by filtration, washed with ethanol, and dried under vacuum. The crystal used in the X-ray structure determination was selected from this sample. Anal. Calcd for $C_{16}H_{18}N_6S_2Fe$: C, 46.38; H, 4.38; N, 20.28; S, 15.48; Fe, 13.48. Found: C, 46.20; H, 4.52; N, 20.01; S, 15.59; Fe, 13.13.

Physical Measurements. Magnetic Measurements. Magnetic susceptibilities were measured in the temperature range 20−300 K with a fully automated Manics DSM-8 susceptometer equipped with a TBT continuous-flow cryostat and a Drusch EAF 16 UE electromagnet operating at ca. 1.7 T. Data were corrected for magnetization of the sample holder and for diamagnetic contributions, which were estimated from the Pascal constants.

Mössbauer Spectra. The variable-temperature Mössbauer measurements were obtained on a constant-acceleration spectrometer with a 25 mCi source of ^{57}Co (Rh matrix). Isomer shift values (IS) are given with respect to metallic iron at room temperature. The absorber was a sample of 100 mg of microcrystalline powder enclosed in a 2 cm diameter cylindrical plastic sample holder, the size of which had been determined to optimize the absorption. Variable-temperature spectra were obtained in the 80−305 K range, by using a MD306 Oxford cryostat, the thermal scanning being monitored by an Oxford ITC4 servocontrol device (±0.1 K accuracy). A least-squares computer program was used to fit the Mössbauer parameters and determine their standard deviations of statistical origin (given in parentheses).[11]

Table 3. Selected Bond Distances (Å) for [Fe(DPEA)(NCS)$_2$][a]

Fe1−N1	2.115(4)	N3−C30	1.353(7)
Fe1−N2	2.155(5)	N3−C34	1.344(6)
Fe1−N3	2.186(4)	C30−C31	1.359(8)
Fe1−N4	2.177(4)	C31−C32	1.349(9)
Fe1−N5	2.231(4)	C32−C33	1.39(1)
Fe1−N6	2.215(5)	C33−C34	1.378(7)
S1−C1	1.690(7)	C34−C35	1.524(8)
N1−C1	1.029(7)	N4−C40	1.341(6)
S2−C2	1.616(5)	N4−C44	1.345(7)
N2−C2	1.151(7)	C40−C41	1.366(9)
N6−C53	1.507(8)	C41−C42	1.38(1)
C53−C52	1.453(9)	C42−C43	1.35(1)
C52−N5	1.480(8)	C43−C44	1.394(9)
N5−C35	1.471(7)	C44−C45	1.495(8)
N5−C45	1.486(8)		

[a] Estimated standard deviations in the least significant digits are given in parentheses.

Table 4. Selected Angles (deg) for [Fe(DPEA) (NCS)$_2$][a]

N1−Fe1−N2	95.6(2)	C52−N5−C35	110.0(4)
N1−Fe1−N6	95.1(2)	C52−N5−C45	114.0(4)
N1−Fe1−N5	174.1(2)	C35−N5−C45	111.0(4)
N1−Fe1−N3	103.5(2)	Fe1−N3−C30	127.0(3)
N1−Fe1−N4	104.2(2)	Fe1−N3−C34	116.2(3)
Fe1−N6	167.4(2)	C30−N3−C34	116.6(4)
N2−Fe1−N5	90.2(2)	N3−C30−C31	123.1(5)
N2−Fe1−N3	93.7(2)	C30−C31−C32	120.3(6)
N2−Fe1−N4	85.6(2)	C31−C32−C33	118.4(6)
N6−Fe1−N5	79.2(2)	C32−C33−C34	118.9(5)
N6−Fe1−N3	90.3(2)	N3−C34−C33	122.7(5)
N6−Fe1−N4	85.3(2)	N3−C34−C35	114.6(4)
N5−Fe1−N3	75.2(1)	C33−C34−C35	122.7(5)
N5−Fe1−N4	77.0(1)	N5−C35−C34	109.6(4)
N3−Fe1−N4	152.2(1)	Fe1−N4−C40	126.1(4)
Fe1−N1−C1	166.2(5)	Fe1−N4−C44	115.0(3)
S1−C1−N1	176.1(6)	C40−N4−C44	119.0(4)
Fe1−N2−C2	158.2(4)	N4−C40−C41	123.1(6)
S2−C2−N2	179.2(5)	C40−C41−C42	117.6(6)
Fe1−N6−C53	108.4(4)	C41−C42−C43	120.4(7)
N6−C53−C52	109.3(5)	C42−C43−C44	119.6(7)
C53−C52−N5	114.0(5)	N4−C44−C43	120.3(5)
Fe1−N5−C52	108.1(3)	N4−C44−C45	117.1(5)
Fe1−N5−C35	106.6(3)	C43−C44−C45	122.5(5)
Fe1−N5−C45	106.7(3)	N5−C45−C44	111.6(5)

[a] Estimated standard deviations in the least significant digits are given in parentheses.

Solution and Refinement of the X-ray Structure. The structure of the above described complex was determined at room temperature (ca. 298 K). The crystal was sealed in a Lindemann capillary and mounted on a four-circle diffractometer (CAD4 Enraf-Nonius) with Cu anticathode and graphite monochromator. Crystal data and refinement results are summarized in Table 1. Cell parameters were determined from 25 reflections with 2θ angles between 6.4 and 51.5°. Three reflections were measured every 1 h as a control of the crystal quality and every 100 reflections as an intensity control. The 7903 reflections were measured and merged ($R = 0.046$). The 3566 unique reflections were used in the refinement. The "SDP"[12] package supplied by Nonius was used to correct the intensities from absorption and usual

(11) Varret, F. *Proceedings of the International Conference on Mössbauer Effect Applications.* Jaipar, India, 1981; Indian National Science Academy: New Delhi, 1982.
(12) Frenz, B. A. *Stucture determination package*; Enraf-Nonius: Delft, The Netherlands, 1982.

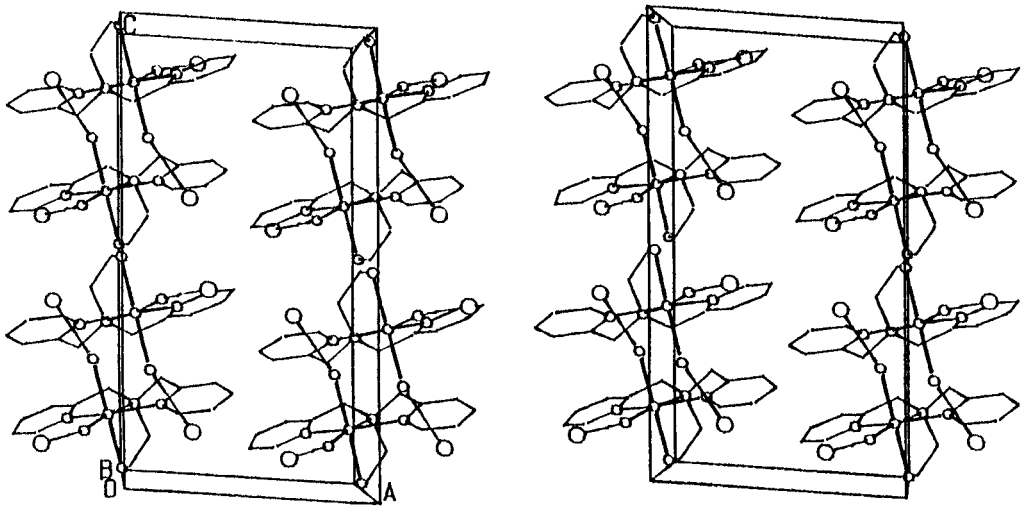

Figure 2. Stereoview of the packing diagram for [Fe(DPEA)(NCS)$_2$].

Lorentz polarization; MULTAN[13] was used to solve the structure by use of direct methods, and the "SHELX-76" program[14] was used for the refinement by full-matrix least-squares methods. Non-hydrogen atoms were refined anisotropically, and all hydrogen atoms were refined isotropically. Hydrogen coordinates, anisotropic thermal parameters of non-hydrogen atoms, remaining bond distances and angles, and least-square planes are deposited as Supporting Information.

Results

Ligand and Complex Syntheses. The new ligand DPEA was obtained in ca. 16% overall yield by the straightforward synthesis shown in Scheme 1. The Schiff base formed in situ from pyridine-2-carboxaldehyde and 2-(aminomethyl)pyridine was reduced to the corresponding amine (DPA) in the presence of zinc powder and acetic acid (40%). Then reaction of DPA with N-(2-bromoethyl)phthalimide followed by hydrazinolysis provided the tetradentate ligand DPEA (41%) as a yellow syrup, essentially pure for the next step. The desired complex [Fe(DPEA)(NCS)$_2$] was obtained by mixing equimolecular amounts of [Fe(py)$_4$(NCS)$_2$] and DPEA in a 2:1 mixture of methanol and ethanol from which crystals suitable for the physical studies were obtained. These crystals were not solvated, and their elemental analysis (C, H, N, S, Fe) was consistent with the expected composition.

Description of the Structure. The complex [Fe(DPEA)(NCS)$_2$] crystallizes in the monoclinic space group $P2_1/c$ ($Z = 4$). The perspective view of the molecule is shown in Figure 1 and corresponds to structure **1** in Chart 1. Fractional atomic coordinates and selected bond lengths and angles are given in Tables 2−4, respectively.

[FeN$_6$] Octahedral Geometry. Two of the six nitrogen atoms coordinated to the Fe(II) center belong to the *cis* thiocyanate groups and four belong to the tetradentate ligand. The latter is coordinated by its two pyridine nitrogen atoms in apical position and by two aliphatic amino groups in adjacent position. The Fe−N distances involving the thiocyanate groups (Fe−N1 = 2.115(4) Å, Fe−N2 = 2.155(5) Å) are shorter than those involving the pyridine rings (Fe−N3 = 2.186(4) Å, Fe−N4 = 2.177(4) Å) and the aliphatic amino groups (Fe−N5 = 2.231(4) Å, Fe−N6 = 2.215(5) Å). The N−Fe−N angles between *cis* nitrogen atoms are found in the range 75.2(1)−104.2(2)°, and those between *trans* nitrogen atoms are in the range 152.2(1)−174.1(2)°; these values strongly deviate from the values of 90 and 180 that would be observed in an ideal octahedron. This severe distortion of the [FeN$_6$] core from O_h symmetry is certainly due to the steric constraints caused by the coordination of the tetradentate ligand. A similar feature has been observed for high-spin complexes [FeL$_2$(NCS)$_2$] containing bidentate ligands.[8g−j,15] The NCS groups are almost linear (N1−C1−S1 = 176.1(6)°, N2−C2−S2 = 179.2(5)°), whereas the Fe−N−C linkages are appreciably bent (Fe−N1−C1 = 166.2(5)°, Fe−N2−C2 = 158.2(4)°).

Stereochemistry. The tetradentate ligand DPEA being coordinated to the iron(II) atom forms three five-membered chelate rings. One of these rings includes the aliphatic ethanediamine fragment; the other two contain the (pyridylmethyl)amino groups of the ligand. Models show that in this octahedral complex the *cis* arrangement of two NCS groups is the only one possible. The pyridine rings of the ligand can have either meridional or facial arrangement (**1** and **2**, respectively, in Chart 1). The facial arrangement leads to a chiral complex (resolvable into enantiomers), whereas the meridional one is achiral. Only complex **1** where the pyridine ligands are meridionally arranged was isolated in this work. This achiral complex shows a residual chirality in the crystal state due to the twist conformation of the five-membered ethanediamine metallocycle, and in the $P2_1/c$ unit cell two pairs of symmetry related left-handed and right-handed conformations exist (Figure 2).

Crystal Packing. Figure 2 displays a stereoview of the crystal structure of **1**. The packing consists of layers of molecules parallel to the *bc* plane. In each layer the cohesion is due to weak hydrogen bonds involving hydrogens H60 and H61 of the amino group N6, which are linked to the thiocyanate sulfur atoms belonging to two different adjacent molecules. Between the layers, in the *a* direction, cohesion is achieved by van der Waals interactions. The hydrogen bonds data and the intermolecular distances shorter than 3.70 Å are listed in Tables 5 and 6, respectively.

Magnetic Susceptibility Data. Variable-temperature magnetic susceptibility data were collected in both cooling and warming modes in the range 20−290 K. The magnetic

(13) Main, P.; Fiske, S. J.; Hull, S. E.; Lessinger, L.; Germain, G.; Declercq, J. P.; Woolfson, M. M. *MULTAN 80, A System of Computer Programs for the Automatic solution of Crystal Structure from X-ray Diffraction Data*; University of York, England, and University of Louvain, Belgium, 1980.

(14) Sheldrick, G. M. *SHELX-76, Computer Program for Crystal Structure Determination*; University of Cambridge: Cambridge, England, 1976.

(15) (a) Roux, C.; Zarembowitch, J.; Gallois, B.; Granier, T.; Claude, R. *Inorg. Chem.* **1994**, *33*, 2273. (b) Real, A.; Zarembowitch, J.; Kahn, O.; Solans, X. *Inorg. Chem.* **1987**, *26*, 2939.

Table 5. Interatomic Distances (Å) and Angles (deg) for the Hydrogen-Bonding Interactions in [Fe(DPEA)(NCS)$_2$][a]

D−H···A	D−H	H···A	D···A	D−H···A
N6−H61···S1[b]	0.76(6)	2.84(6)	3.58(1)	165(5)
N6−H60···S2[b]	0.95(5)	2.63(6)	3.51(2)	156(5)

[a] Estimated Standard deviations in the least significant digits are given in parentheses. [b] Symmetry operations: N6···S1, $-x, -y, -z+1$; N6···S2, $+x, -y+{}^1/_2, +z+{}^1/_2$.

Table 6. Intermolecular Contacts (Å) shorter than 3.70 Å[a]

atoms	sym operators	translations	dist
C1···N6	$-x, -y, -z$	0, 0, 1	3.47(1)
C1···C35	$-x, +y+{}^1/_2, -z+{}^1/_2$	0, −1, 0	3.68(1)
N2···C45	$-x, +y+{}^1/_2, -z+{}^1/_2$	0, −1, 0	3.43(1)
C31···C43	$-x, +y+{}^1/_2, -z+{}^1/_2$	0, −1, 0	3.65(1)
C33···C43	$-x, +y+{}^1/_2, -z+{}^1/_2$	0, −1, 0	3.66(1)
C32···C43	$-x, +y+{}^1/_2, -z+{}^1/_2$	0, −1, 0	3.59(1)
S2···C53	$+x, -y+{}^1/_2, +z+{}^1/_2$	0, 0, −1	3.62(1)
S2···C40	$+x, -y+{}^1/_2, +z+{}^1/_2$	0, 0, −1	3.57(1)
C32···C40	$+x, +y, +z$	−1, 0, 0	3.61(1)
C33···C40	$+x, +y, +z$	−1, 0, 0	3.62(1)
C33···C41	$+x, +y, +z$	−1, 0, 0	3.62(1)
C41···C42	$-x, -y, -z$	1, 1, 1	3.60(1)
C42···C42	$-x, -y, -z$	1, 1, 1	3.65(1)

[a] Estimated standard deviations in the least significant digits are given in parentheses.

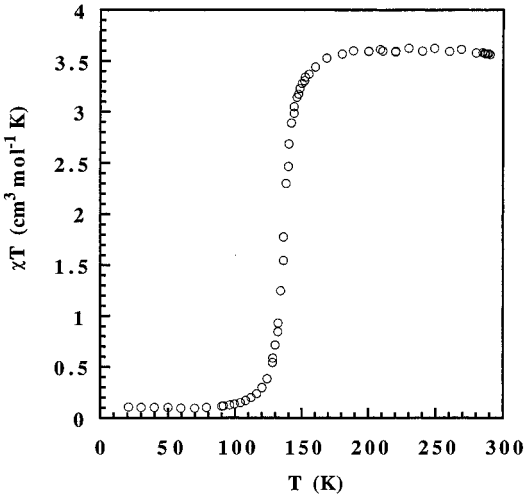

Figure 3. Thermal variation of $\chi_M T$ for [Fe(DPEA)(NCS)$_2$].

properties of complex **1** in the form of $\chi_M T$ vs T are presented in Figure 3. The magnetic measurements revealed a relatively abrupt spin transition between the high spin ($S = 2$) and low spin ($S = 0$) states of the complex. At room temperature (290 K) the magnitude of $\chi_M T$ (3.56 cm^3 mol^{-1} K; $\mu_{eff} = 5.36\ \mu_B$) corresponds to a quintet spin state. This value slowly decreases upon cooling to 150 K, the sharp spin conversion occurring between 150 and 130 K. The spin transition temperature $T_{1/2}$ (temperature for which the high-spin fraction is equal to 0.5) is found at 138 K, with 55% of the spin transition taking place within 10 K (140−130 K). This magnetic behavior implies that a relatively high cooperativity between molecules exists in the crystal. At low temperature (20 K) the value $\chi_M T$ reaches 0.1 cm^3 mol^{-1} K ($\mu_{eff} = 0.89\ \mu_B$), which is close to the temperature-independent paramagnetism value expected for low-spin iron(II) complexes. Although this value could also be explained by the presence of about 2.5% of high-spin iron(II) fraction, the absence of residual paramagnetism at low temperature revealed by Mössbauer spectroscopy (*vide infra*) as well as the closeness of experimental $\chi_M T$ to the expected value for a pure singlet spin state suggests that the spin transition is indeed quasi

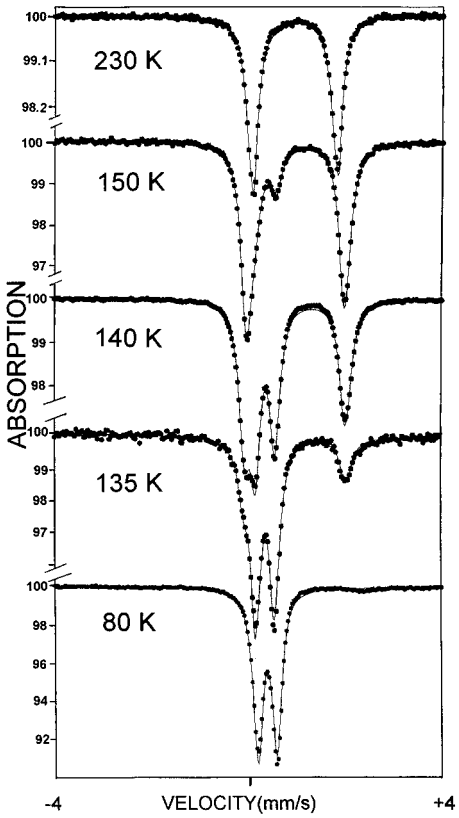

Figure 4. Selected Mössbauer spectra of [Fe(DPEA)(NCS)$_2$] obtained in the cooling mode. The solid lines represent fitted curves.

complete. In the warming mode the same magnetic behavior as in the cooling one was observed and no thermal hysteresis was detected.

Mössbauer Spectroscopy. The Mössbauer studies were performed between 80 and 305 K. Representative Mössbauer spectra of [Fe(DPEA)(NCS)$_2$] obtained in the heating mode are shown in Figure 4. The low- and the high-temperature main doublets are typical for high-spin and low-spin iron(II), respectively. The isomer shift (IS) values are 0.507(7) mm s^{-1} at 80 K and 1.169(1) mm s^{-1} at 305 K. The quadrupole splitting (ΔE_Q) values are in agreement with those previously observed for iron(II) spin-crossover compounds.[1b] At intermediate temperatures the contributions of the two spin states are well resolved and the spectra consist of two doublets in thermal equilibrium with each other. No spectrum deformation or line broadening was observed in this temperature range (80−305 K), indicating that the LS ⇌ HS conversion rates are slow compared to the hyperfine frequencies ($\sim 10^8$ s^{-1}).[16] The 80 K spectrum evidences the absence of residual high-spin fraction, while the 305 K spectrum indicates the presence of a small residual low-spin fraction (6(1)%). Detailed values of the Mössbauer parameters resulting from the least-squares fitting procedures are listed in Table 7 for a representative set of temperatures.

The n_{HS} values obtained through magnetic susceptibility measurements were calibrated with the 293 K $n_{HS}(\sim A_{HS}/A_{tot})$ value obtained from the Mössbauer measurements. The thermal variation of n_{HS} resulting from the magnetic susceptibility measurements (see Figure 5) agrees perfectly with that obtained from the Mössbauer study. Figure 5 clearly shows that the spin-state conversion is relatively steep and achieved essentially

(16) (a) Adler, P.; Hauser, A.; Vefn, A.; Spiering, H.; Gütlich, P. *Hyperfine Interact.* **1989**, *47*, 343. (b) Adler, P.; Spiering, H.; Gütlich, P. J. *Chem. Phys. Lett.* **1994**, *226*, 289.

Table 7. Least-Squares-Fitted Mössbauer Data[a,b] for [Fe(DPEA)(NCS)$_2$]

	low-spin state			high-spin state			
T (K)	IS (mm s^{-1})	ΔE_Q^{LS} (mm s^{-1})	$\Gamma/2$ (mm s^{-1})	IS (mm s^{-1})	ΔE_Q^{HS} (mm s^{-1})	$\Gamma/2$ (mm s^{-1})	A_{HS}/A_{tot} (%)
80	0.505(1)	0.382(1)	0.115(1)				0
135	0.488(1)	0.378(2)	0.117(1)	1.073(4)	2.04(1)	0.135(6)	23
140	0.487(1)	0.390(2)	0.119(1)	1.079(1)	2.000(2)	0.137(2)	51
150	0.462(3)	0.413(4)	0.126(3)	1.073(1)	1.951(2)	0.136(1)	80
230	*0.375*	*0.4*	0.23(5)	1.032(1)	1.687(2)	0.126(1)	95

[a] IS, isomer shift; ΔE_Q, quadrupole splitting; Γ, half-height width of the line; A_{HS}/A_{tot}, area ratio. [b] With their statistical standard deviations given in parentheses; italicized values were fixed to the fit; isomer shift values refer to metallic iron at 300 K. *A*: base-line-corrected data area.

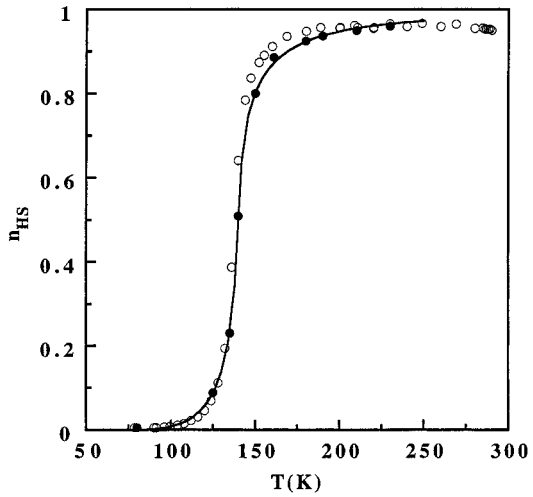

Figure 5. Thermal variation of the high-spin fraction (n_{HS}) of [Fe(DPEA)(NCS)$_2$]. Open and black circles correspond to magnetic susceptibility and to Mössbauer spectroscopy data, respectively. The solid line represents a least-squares fit with the two-level Ising-like model.

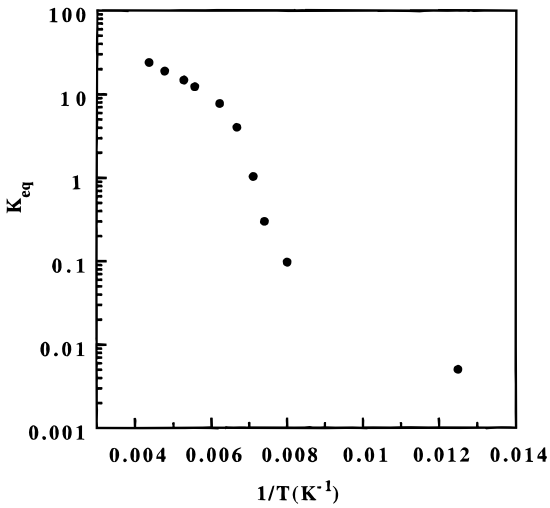

Figure 6. Arrhenius plot of the eqilibrium constant obtained by Mössbauer spectroscopy for [Fe(DPEA)(NCS)$_2$].

between 130 and 150 K. The spin transition temperature, $T_{1/2}$, is close to 138 K. The transition temperature $T_{1/2}$ found from the Mössbauer spectroscopy is identical with that given by magnetic measurements.

Discussion

The new spin transition complex [Fe(DPEA)(NCS)$_2$] (**1**) illustrates the interest of using ligands that combine aliphatic and aromatic nitrogen donor atoms in their structure to design compounds presenting spin-state transformations. Numerous complexes with bidentate,[17] tridentate,[18] tetradentate,[9] and hexadentate[1d,5] ligands that meet this requirement have been described. The [Fe(DPEA)(NCS)$_2$] complex discussed here is the first structurally characterized representative of the family of Fe(II) *cis*-diisothiocyanato complexes with tetradentate ligands.[9] The *cis* configuration of the NCS groups is required to avoid the important strain that would result from three meridionally fused chelates. Among diisothiocyanatoiron(II) spin transition complexes only two examples of *trans* NCS groups are known, one with monodentate ligands[15a] and another with bidentate bridging ligands.[19] Nevertheless, there is still some strain in the [Fe(DPEA)(NCS)$_2$] complex, as judged from the opening of the Fe(NCS)$_2$ angle (95.6(2)°) with respect to a value close to 90° that would be expected in an unstrained complex.

A series of *cis*-diisothiocyanatoiron(II) complexes with tetradentate ligands of the bis(2-pyridylmethyl)diamine and tris(2-pyridylmethyl)amine (TPA) types has been described by Toftlund et al.[9] These complexes display either temperature-dependent spin equilibrium ($^5T_2 \rightleftharpoons {}^1A_1$) or a temperature-independent spin state (high spin or intermediate). In the last case the high-spin state is stabilized by the presence in the ligands of methyl substituents in proximity of the nitrogen donor atoms. The TPA ligand differs from the DPEA ligand by the replacement of a 2-aminoethyl group by a 2-pyridylmethyl fragment. The magnetic behavior of the [Fe(TPA)(NCS)$_2$] complex in the temperature range 77−300 K is characterized by a gradual conversion from high to low spin starting immediately below room temperature, whereas for the present [Fe(DPEA)(NCS)$_2$] complex there is no noticeable increase of the low-spin state fraction down to about 170 K. This is certainly in line with the decrease of the ligand field strength in DPEA due to the substitution of one aliphatic nitrogen atom for an aromatic one in the TPA ligand, resulting in a 2:2 aliphatic:aromatic ratio in the former vs 1:3 in the latter. The much more abrupt character of the spin transition in [Fe(DPEA)(NCS)$_2$] than in [Fe(TPA)(NCS)$_2$] indicates that a higher degree of cooperativity exists in the former. The Arrhenius plot of the equilibrium constant ($K_{eq} = n_{HS}/(1 - n_{HS})$) obtained from Mössbauer spectroscopy for [Fe(DPEA)(NCS)$_2$] is shown in Figure 6. It can be clearly seen that the spin conversion is cooperative. The reversed S shape observed is a signature of the departure from an ideal solution behavior (linear plot).[20] The data assembled in Tables 5 and 6 show that, among the six

(17) (a) Renovitch, G. A.; Baker, W. A. *J. Am. Chem. Soc.* **1967**, *89*, 6377. (b) Baker, A. T.; Goodwin, H. A. *Austr. J. Chem.* **1984**, *37*, 1157.
(18) (a) Boylan, M. J.; Nelson, S. M.; Deeney, F. A. *J. Chem. Soc. A* **1971**, 976. (b) Goodwin, H. A.; Mather, D. W. *Austr. J. Chem.* **1974**, *27*, 965. (c) König, E.; Ritter, G.; Irler, W.; Goodwin, H. A. *J. Am. Chem. Soc.* **1980**, *102*, 4681. (d) König, E.; Ritter, G.; Kulshreshtha, S. K.; Waigel, J.; Goodwin, H. A. *Inorg. Chem.* **1984**, *23*, 1896.
(19) (a) Vreugdenhil, W.; Haasnoot, J. G.; Kahn, O.; Thuery, P.; Reedijk, J. *J. Am. Chem. Soc.* **1987**, *109*, 5272. (b) Vreugdenhil, W.; Diemen, J. H.; Graaff, R. A. G. de; Haasnoot, J. G.; Reedijk, J.; Kraan, A. M. van der; Kahn, O.; Zarembowitch, J. *Polyhedron* **1990**, *9*, 2971.
(20) Lemercier, G.; Bousseksou, A.; Seigneuric, S.; Varret, F.; Tuchagues, J. P. *Chem. Phys. Lett.* **1994**, *226*, 289.

nitrogen atoms connected to the metal center, only the aliphatic ones N2 and N6 participate in the intermolecular interactions, the pyridinic N3 and N4 being protected by the aromatic rings. The hydrogen bonds involving the N6 atom, which cannot occur in the [Fe(TPA)(NCS)$_2$] complex, possibly represent the most important channel responsible for the cooperativity in complex **1**, others being provided by the intermolecular C···C contacts. We also suspect that the flexibility of the ligand amino aliphatic chain can contribute to the cooperativity effects.

The n_{HS} fraction obtained from Mössbauer data could be fitted by the mean-field equation of the two level Ising-like model[7] formally equivalent to the macroscopic model[4f,21] (Figure 5). The parameter values for the best least-squares fit are $\Delta_{eff} = 835$ K, $J_{coop} = 124$ K, and $r_{eff} = 391$; J_{coop} is the ferromagnetic-like intermolecular coupling parameter (cooperativity parameter),[7] $\Delta_{eff} = E_{HS} - E_{LS}$ is the energy splitting of two levels of a fictious spin ± 1, and $r_{eff} = g_{HS}/g_{LS}$ is the ratio of effective degeneracies of electron−vibrational levels in high-spin and low-spin states.[4f,21] With the values of the parameters r_{eff} and Δ_{eff} and using the formal relationship between the macroscopic (entropy and enthalpy) and microscopic parameters (Δ_{eff} and r_{eff}), we can thus estimate the molar entropy and enthalpy changes upon spin-state conversion as $\Delta S = R \ln r_{eff} = 49$ J K^{-1} mol^{-1} and $\Delta H = N\Delta_{eff} = 6.76$ kJ mol^{-1}.

The calculated variations of enthalpy and entropy fall within the limits $\Delta H \approx 6-15$ kJ mol^{-1} and $\Delta S \approx 37-65$ J K^{-1} mol^{-1} found for mononuclear iron(II) spin transition compounds from calorimetric measurements.[1e,g] In spite of the absence of thermal hysteresis, evidenced by the magnetic measurements in cooling and heating modes, the value of the ratio $J_{coop}/T_{1/2} = 0.9$ indicates that the spin-state conversion in **1** is close to a first-order spin-state transition for which $J_{coop}/T_{1/2} = 1$.[22] It suggests that small structural or chemical modifications of the [Fe(DPEA)(NCS)$_2$] complex could lead to a first-order transition. Studies of new systems that involve either modifications of the polydentate ligand or replacement of the two NCS groups by bidentate ligands are in progress.

Acknowledgment. We are grateful to the CNRS, Département des sciences chimiques, for a grant to G.M.

Supporting Information Available: A full presentation of crystallographic data and experimental parameters for [Fe(DPEA)(NCS)$_2$] (Table S1), general displacement parameter expressions, B's (Table S2), positional parameters and isotropic displacement parameters for the hydrogen atoms (Table S3), bond distances and angles (Tables S4 and S5, respectively), and least-squares planes (Table S5) (6 pages). Ordering information is given on any current masthead page.

IC9615133

(21) (a) Bousseksou, A.; Nasser, J.; Linares, J.; Boukheddaden, K.; Varret, F. *Mol. Cryst. Liq. Cryst.* **1993**, *243*, 269. (b) Bousseksou, A. Ph.D. Thesis, Université Paris 6, 1992.

(22) Wajnflasz, J.; Pick, R. *J. Phys. C* **1971**, *32*, 1.